Applied Magnetic Resonance 2, 441–463 (1991)

Applied Magnetic Resonance

Knight Shift Tensors and π-Spin Densities in the Organic Metals α_t-(BEDT-TTF)$_2$I$_3$ and (BEDT-TTF)$_2$Cu(NCS)$_2$

T.Klutz[1], I.Hennig[1], U.Haeberlen[1] and D.Schweitzer[2]

[1] Max-Planck-Institut für Medizinische Forschung, Arbeitsgruppe Molekülkristalle, Heidelberg, Germany
[2] 3. Physikalisches Institut, Universität Stuttgart, Stuttgart, Germany

Received April 12, 1991

Abstract. ^{13}C-MASS spectra of pure BEDT-TTF and of the organic metals α_t-(BEDT-TTF)$_2$I$_3$ and (BEDT-TTF)$_2$Cu(NCS)$_2$ were recorded at ν_L = 68 MHz. Isotropic shifts and the principal components of the shift tensors were determined, respectively, from the center and spinning side bands. For pure BEDT-TTF which is a diamagnetic insolator, the measured shifts are *chemical* shifts while for the organic metals they are the sum of chemical and Knight shifts. In each of the compounds the shifts are assigned in *groups* to the *inner, middle* and *outer* carbons of the BEDT-TTF molecule. For the organic metals the separation of the experimental shifts into chemical and Knight shifts is discussed. From the anisotropic part of the Knight shift tensors the π-spin densities at the carbon and sulphur positions of the BEDT-TTF molecule are inferred. The result is that the π-spin density of the unpaired hole is concentrated on the center part of the BEDT-TTF molecule, i.e., on the inner and middle carbons, and on the inner sulphurs. It is argued that the current density is concentrated on this part of the BEDT-TTF molecule as well.

1. Introduction

Radical salts of BEDT-TTF are crystalline solids which consist of two components: the organic BEDT-TTF (bisethylenedithiolotetrathiafulvalene) cations and "small" inorganic anions. The BEDT-TTF-molecule is shown in Fig.1. In this figure we introduce the notation for the carbon and sulphur positions we are going to use in this paper. C_i, C_m and C_o stand, respectively, for the inner, middle and outer carbon atoms which can be distinguished in a ^{13}C-spectrum of dissolved BEDT-TTF, and S_i, S_o for the inner and outer sulphur atoms. BEDT-TTF forms quasi-two-dimensional organic metals with a variety of different anions, e.g., I_3^-, $IAuI^-$ and $Cu(NCS)_2^-$. The momentary symmetry of the isolated BEDT-TTF molecule is S_2, i.e., there is an inversion center in the middle of the molecule. In solution the molecule is flexible and on the time

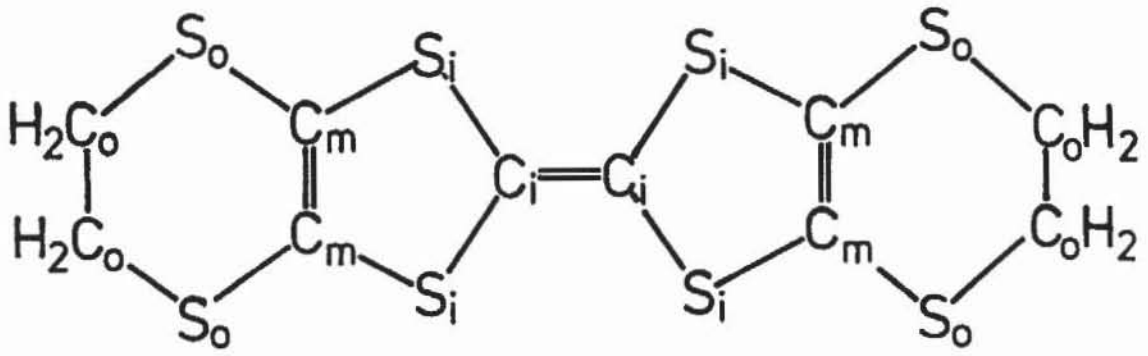

Fig.1. The BEDT-TTF molecule. Here we introduce the notation C_i, C_m and C_o for the inner, middle and outer carbons and S_i, S_o for the inner and outer sulphurs.

average the symmetry is D_{2h}. All these molecular symmetry elements are lost upon incorporation of the molecule in crystals of either pure or radical salts of BEDT-TTF.

The electrochemical preparation of BEDT-TTF with I_3^- counterions yields two radical salts with identical stoichiometries but different structures. These two salts are the so-called α- and β-(BEDT-TTF)$_2$I$_3$ phases [1—3]. Crystals of the α-phase are usually plate-like while β-phase crystals are canted rhombohedrons. α-(BEDT-TTF)$_2$I$_3$ is a two-dimensional organic metal at room temperature with a metal insulator transition at 135 K [1,2]. Crystals of β-(BEDT-TTF)$_2$I$_3$ are also two-dimensional metals but stay metallic upon cooling and become superconducting at $T_c = 1.3$ K [3].

Another superconductor on the basis of BEDT-TTF and I_3 can be obtained by tempering crystals of α-(BEDT-TTF)$_2$I$_3$ for several days at about 70°C [4,5]. The resulting crystals, called α_t-(BEDT-TTF)$_2$I$_3$, become superconducting at $T_c = 8$ K [5]. A detailed X-ray structure determination of α_t-(BEDT-TTF)$_2$I$_3$ was not possible up to now due the fact that during the structural transformation the mechanically still very stable crystals acquire a mosaic structure. However, it could be shown by several spectroscopic methods, especially ^{13}C-NMR, that the structure of α_t-(BEDT-TTF)$_2$I$_3$ is very similar to that of β-(BEDT-TTF)$_2$I$_3$ [6]. In all these crystals the BEDT-TTF-molecules form two-dimensional conducting sheets [7—9]. Short intermolecular sulphur-sulphur distances within these sheets result in an overlap of p-orbitals centered om sulphur atoms of different BEDT-TTF molecules. The contacts established in this way between the BEDT-TTF molecules are thought to be responsible for the conductivity. The conducting sheets are separated by layers of I_3^- anions. The conductivity at room temperature is nearly isotropic within the sheets, the largest observed values are 250 S/cm for the α- and 50 S/cm for the α_t- and β-phases. The conductivity is about 1000 times smaller along the direction perpendicular to the sheets.

(BEDT-TTF)$_2$Cu(NCS)$_2$ is metallic at room temperature and becomes superconducting at $T_c = 10.4$ K [10,11]. The BEDT-TTF molecules form dimers.

There are two dimers per unit cell which are nearly perpendicular to each other. The dimers form two-dimensional conducting sheets. Contacts between molecules are again established by short intermolecular sulphur-sulphur distances.

In this paper we report on ^{13}C-MASS spectra registered at room temperature of pure BEDT-TTF, α_t-(BEDT-TTF)$_2$I$_3$ and (BEDT-TTF)$_2$Cu(NCS)$_2$. We use these spectra for inferring the π-spin densities of the unpaired electron on the BEDT-TTF molecule in the two organic metals. These π-spin densities allow us to visualize the path which the charge carriers take through the crystal. To determine the distribution of the π-spin density from ^{13}C-spectra the following steps are necessary: i) The ^{13}C-resonances must be assigned to the different carbon positions of the molecule. A serious problem we encounter at this stage is the fact that the C_2-axes as well as the inversion center in the middle of the isolated molecule are lost upon incorporation of the molecule into the crystal. This means that in our spectra we get *two* different lines from the inner and *four* different lines from both the middle and the outer carbons. The basic difficulty is that we cannot distinguish between the carbons within a particular group. This forces us to use *average* shift tensors for the groups of inner, middle and outer carbons. This is the decisive point because it determines the uncertainties of the inferred π-spin densities. ii) The next step is to determine the principal values of the ^{13}C shift tensors from the intensities of the spinning sidebands. iii) We then must separate the measured shifts into chemical and Knight shifts. iv) Finally we must relate the Knight shift tensors to the π-spin densities. The contribution to the Knight shift of a carbon k from the π-spin density $\varrho_{\pi c_k}$ on this very carbon is proportional to $\chi^{(s)} \cdot \varrho_{\pi c_k}$, where $\chi^{(s)}$ is the Pauli susceptibility of the compound. The susceptibilities of α_t-(BEDT-TTF)$_2$I$_3$ and (BEDT-TTF)$_2$Cu(NCS)$_2$ are known from measurements by Klotz *et al.* [12] and Urayama *et al.* [13]. The constant of proportionality can be calculated from the field an unpaired electron in a $2p_z$ orbital produces at the site of the carbon. This Knight shift contribution is necessarily axially symmetric. The Knight shift contributions from π-spin densities on neighbouring nuclei can be accounted for with sufficient accuracy by assuming that the π-spin densities on these nuclei are concentrated at the sites of these nuclei (point dipole approximation). These contributions are responsible for (small) deviations of the total Knight shift tensors from axial symmetry.

Knight shifts and π-spin densities have been determined previously in β-(BEDT-TTF)$_2$I$_3$ by Vainrub *et al.* [14] and in two radical salts of fluoranthene, which are also organic metals, by Mehring and Spengler [15], Stöcklein *et al.* [16] and Wind *et al.* [17]. The methods used in all of these studies for extracting the π-spin densities from the directly observed quantities differ, however, from ours. ^{13}C and ^{63}Cu Knight shifts in the organic metal (2,5-dimethyl-dicyanoquinonediimine)$_2$Cu were reported by Köngeter *et al.* [18] while the ^{13}C Knight shifts in a representative, (TMTSF)$_2$ClO$_4$, of the TMTSF class of organic metals were measured by Bernier *et al.* [19].

2. The Crystal Structures of BEDT-TTF and its Radical Salts with I_3^- and $Cu(NCS)_2^-$

In this section we discuss briefly the crystal structures of the BEDT-TTF radical salts investigated in this work to evaluate the number of ^{13}C lines in a ^{13}C-MASS spectrum, i.e., to evaluate the complexity of the task we are undertaking.

Crystals of pure BEDT-TTF are insulators. Their space group is $P2_1/c$. There are four BEDT-TTF-molecules in the unit cell which are pairwise arranged as dimers. The two molecules of a dimer are related by an inversion center, i.e., they are magnetically equivalent. The dimers are related by a two-fold screw axis, i.e., all four molecules in the unit cell are crystallographically equivalent [20]. As crystallographically equivalent nuclei give identical resonances in a ^{13}C-MASS spectrum the ^{13}C-MASS spectrum of pure BEDT-TTF will consist of ten ^{13}C-resonances corresponding to the ten inequivalent carbon positions of one BEDT-TTF molecule.

The space group of β-$(BEDT\text{-}TTF)_2I_3$ is also $P\bar{1}$. The crystal structure is shown in Fig.2. As mentioned before the same space group and structure also apply for α_t-$(BEDT\text{-}TTF)_2I_3$. The unit cell holds two BEDT-TTF molecules which are related by the inversion center [7,8]. Therefore all molecules are magnetically equivalent. In a ^{13}C-MASS spectrum we expect ten ^{13}C-resonances.

The space group of the organic superconductor $(BEDT\text{-}TTF)_2Cu(NCS)_2$ is $P2_1$. There are four BEDT-TTF molecules in the unit cell which are all magnetically inequivalent. Pairs of molecules are related by the two-fold screw axis and are therefore crystallographically equivalent [9]. In a ^{13}C-MASS spectrum twenty ^{13}C-resonances are expected from two BEDT-TTF molecules.

3. Experimental

^{13}C-MASS spectra were recorded by Fourier transform NMR at room temperature on a homebuilt spectrometer operating at 68 MHz, corresponding to a field of 6.4 Tesla. A double bearing rotor with a diameter of 7 mm was used. The samples consisted of a finely ground powder of the respective material. Of the two radical salts we also prepared samples in which the inner and middle, but not the outer carbon positions were 10 % ^{13}C-enriched. The enrichment was deliberately restricted to 10 % to avoid line broadening in the ^{13}C-spectra by ^{13}C–^{13}C dipole-dipole coupling. Spectra were either recorded by ^1H–^{13}C cross polarization or by direct excitation with an rf pulse. When we wanted to study all resonances we used cw proton decoupling during acquisition of the ^{13}C FID. When no cw proton decoupling is applied

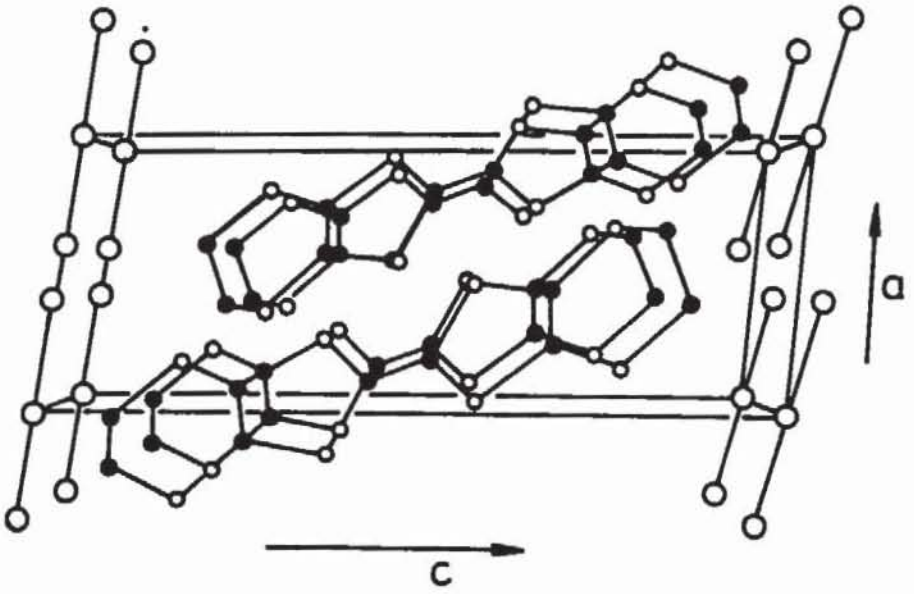

Fig.2. The structure of β-(BEDT-TTF)$_2$I$_3$ viewed along the *b*-axis.

only the resonances of the inner and middle carbons appear in the spectra because the resonances of the outer carbons to which two protons are directly bonded are then broadened so much that they disappear in the noise. To distinguish the central lines of the MASS spectra from the spinning sidebands we recorded spectra at different spinning frequencies and cross checked the results with spectra recorded with one of the six-pulse TOSS sequences proposed by Raleigh *et al.* [21]. Spinning frequencies ν_R of 4–5 kHz were used when attention was focused on the central lines whereas ν_R was chosen in the range of 2–3 kHz for determining the principal values of the shift tensors from the intensities of the sidebands.

4. Results

4.1. ^{13}C-MASS Spectra and Assignment of Resonances

In Fig.3 we show ^{13}C-MASS spectra from BEDT-TTF, α_t-(BEDT-TTF)$_2$I$_3$ and (BEDT-TTF)$_2$Cu(NCS)$_2$. The central lines are marked by arrows. The spectrum of BEDT-TTF was recorded with cross-polarization and cw-^{1}H-decoupling. The mixing time was 6 ms, the number of accumulations 5000. The decoupling power corresponded to a 90°-rf-pulse of 4 μs duration. BEDT-TTF is an insulator therefore the resonances are determined by the *chemical* shifts. As explained in Section 2 the spectrum of BEDT-TTF should consist of ten ^{13}C-resonances. The blow ups on the top of Fig.3 demonstrate that all ten resonances can indeed be resolved. We assign the resonances in the following way to the carbon positions:

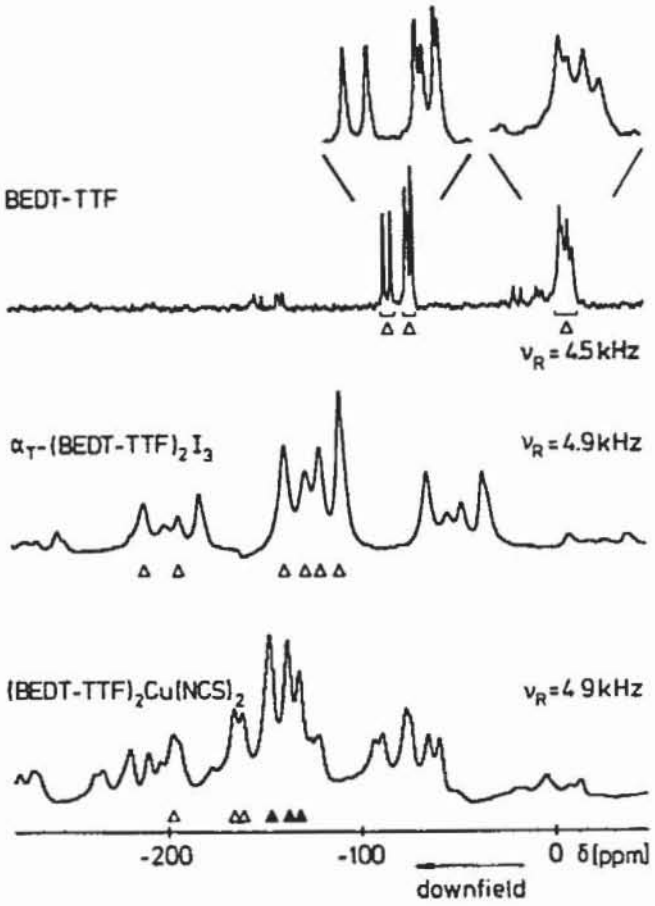

Fig.3. ^{13}C-MASS spectra of pure BEDT-TTF, α_t-(BEDT-TTF)$_2$I$_3$ and (BEDT-TTF)$_2$Cu(NCS)$_2$ taken at ν_L = 68 MHz and room temperature. The spectrum of pure BEDT-TTF was recorded by ^{1}H–^{13}C crosspolarization and proton decoupling whereas the spectra of α_t-(BEDT-TTF)$_2$I$_3$ and (BEDT-TTF)$_2$Cu(NCS)$_2$ were recorded by direct excitation and without proton decoupling. The shifts are referenced to TMS.

The four resonances at $\bar{\sigma} \approx 0$ ppm are assigned to the *outer*, those at $\bar{\sigma} \approx -80$ ppm to the *middle* and the two resonances at $\bar{\sigma} \approx -90$ ppm to the *inner* carbons.

This assignment is based on the following arguments: The width of the lines of the group of resonances at $\bar{\sigma} \approx 0$ ppm is very sensitive to the frequency and to the power of the decoupling irradiation. This behaviour is expected only for the resonances of the outer carbons to each of which two hydrogens are bonded. The *number of resonances* in the two distinctly different groups of lines at $\bar{\sigma} \approx -80$ ppm (four lines) and $\bar{\sigma} \approx -90$ ppm (two lines) allows to distinguish resonances from the inner from those of the middle carbons: there are *four* middle but only *two* inner carbons. As mentioned in the introduction it is not possible to assign the individual resonances within the groups of lines to individual carbons.

^{13}C-MASS spectra from the ^{13}C-enriched samples of α_t-(BEDT-TTF)$_2$I$_3$ and (BEDT-TTF)$_2$Cu(NCS)$_2$ are shown in the center and bottom of Fig.3. These spectra were recorded without ^{1}H–^{13}C cross polarization and without

^{1}H-decoupling. They were excited in a straightforward manner with $\pi/2$-pulses. The number of accumulations was 60000. The ^{13}C spin lattice relaxation time of the C_i and C_m carbons was measured and found to be about $T_1^{(i)} = 30$ ms and $T_1^{(m)} = 120$ ms for α_t-(BEDT-TTF)$_2$I$_3$ and $T_1^{(i)} = 90$ ms and $T_1^{(m)} = 140$ ms for (BEDT-TTF)$_2$Cu(NCS)$_2$. Therefore the waiting time between pulses could be chosen as short as 100 ms. The resonances from the outer carbons C_o are suppressed in these spectra for the following three reasons: i) only the C_i and C_m carbon positions were tenfold ^{13}C-enriched in the respective samples; ii) the spin lattice relaxation time of the C_o carbons is about 500 ms so that during signal accumulation with a pulse repetition time of 100 ms the C_o resonances are substantially saturated; iii) the absence of ^{1}H-decoupling irradiation causes the resonances of the outer carbons, to each of which two hydrogens are bonded, to become smeared out over a large spectral range. We point out that the widths of the resonances of the inner and middle carbons, which are substantially larger than in the spectrum of pure BEDT-TTF, are not caused by the lacking ^{1}H-decoupling. The coupling of these carbons to the (distant) protons is so weak that it does not affect the linewidths on the level of resolution achieved in the spectra of the organic metals shown in Fig.3. We suspect that the linewidths in these spectra are dominated by the electronic paramagnetism of the conducting radical salts. However, ^{13}C—^{13}C dipole-dipole coupling may also contribute somewhat to the linewidths.

As expected from the crystal structure we observe $10-4 = 6$ central resonances in the spectrum of α_t-(BEDT-TTF)$_2$I$_3$. In the spectrum of (BEDT-TTF)$_2$Cu(NCS)$_2$ some of the resonances coincide which can be seen by a comparison of the intensities of the lines. Remember that the intensity of each central line including the respective sidebands must be equal for all carbon positions. In Fig.3 single resonances are marked with open and triple resonances with full arrows. According to this counting the resonances of *twelve* carbons are indeed observed in the spectrum of (BEDT-TTF)$_2$Cu(NCS)$_2$.

The resonances in the spectrum of α_t-(BEDT-TTF)$_2$I$_3$ clearly come in two groups and can be assigned by their number: The group of *two* resonances is assigned to the *inner*, the group of *four* lines to the *middle* carbons. This implies that the inner carbons experience the largest downfield shifts.

For (BEDT-TTF)$_2$Cu(NCS)$_2$ the resonances of the inner and middle carbons do not come in two clearly distinct groups, see Fig.3 bottom. The comparison with the spectrum of α_t-(BEDT-TTF)$_2$I$_3$ suggests that the group of resonances at $\bar{\sigma} \approx -140$ ppm arises from the *middle* while the resonances with the larger downfield shifts arise from the *inner* carbons. As there are *four* inner and *eight* middle carbons in (BEDT-TTF)$_2$Cu(NCS)$_2$ the resonances of one inner carbon must essentially coincide with two coinciding resonances of middle carbons. Since the resonances of the inner and middle

carbons are clearly distinct and reliably assignable for α_t-(BEDT-TTF)$_2$I$_3$ but not for (BEDT-TTF)$_2$Cu(NCS)$_2$ we concentrate in what follows on α_t-(BEDT-TTF)$_2$I$_3$.

4.2. The Anisotropic Parts of the Shift Tensors

To determine the principal values of the ^{13}C shift tensors $\boldsymbol{\delta}$ in pure BEDT-TTF, α_t-(BEDT-TTF)$_2$I$_3$ and (BEDT-TTF)$_2$Cu(NCS)$_2$ we have analyzed the intensities of the sidebands in the respective MASS-spectra. In each case the outer carbons of the BEDT-TTF molecule have no spinning sidebands for spinning frequencies $\nu_R \geqq 2$ kHz, i.e., the anisotropy $\Delta\delta$ of $\boldsymbol{\delta}$ is small: $\Delta\delta$(outer carbons)$\leqq(\nu_R/\nu_L) \simeq 30$ ppm. By contrast, the inner and middle carbons produce strong sidebands. As an example we have marked in Fig.4 the sidebands of one of the middle carbons together with their relative intensities. Using the graphical methods described by Herzfeld and Berger [22] we determined the principal values δ_{xx}, δ_{yy} and δ_{zz} of the shift tensors $\boldsymbol{\delta}$ of the inner and middle carbons from these intensity ratios. The results obtained for pure BEDT-TTF and α_t-(BEDT-TTF)$_2$I$_3$ are presented in Table 1. The errors limits $\Delta\delta_{\alpha\alpha}$, $\alpha = x,y,z$ given in this Table for the *individual* carbons originate from the uncertainty with which the intensities of the spinning sidebands could be determined. The error limits given for the principal components of the *average* shift tensors $\langle\boldsymbol{\delta}^{(c)}\rangle_{av}$, c = i,m, were calculated according the following *ad hoc* rule: from the errors $\Delta\delta_{\alpha\alpha}$ of the individual carbons an average error $\langle\Delta\delta^{(c)}_{\alpha\alpha}\rangle_{av}$ was calculated according to the error propagation law, $\langle\Delta\delta^{(c)}_{\alpha\alpha}\rangle_{av} = [\sum_\alpha(\Delta\delta_{\alpha\alpha})^2]^{1/2}$. In addition, the maximum of $|\langle\delta^{(c)}_{\alpha\alpha}\rangle_{av} - \delta^{(c)}_{\alpha\alpha,individual}|$, called $\Delta^{(c)}_{\alpha\alpha,max}$ was calculated for $\alpha = x,y,z$ and c = i and m. The error of $\langle\delta^{(c)}_{\alpha\alpha}\rangle_{av}$ given in Table 1 is the *larger* of the two numbers $\Delta^{(c)}_{\alpha\alpha,max}$ and $\langle\Delta\delta^{(c)}_{\alpha\alpha}\rangle_{av}$.

For (BEDT-TTF)$_2$Cu(NCS)$_2$ we confine ourselves to summarizing the principal components of $\langle\boldsymbol{\delta}^{(i)}\rangle_{av}$ and $\langle\boldsymbol{\delta}^{(m)}\rangle_{av}$ and their error limits in Table 2.

Table 1. Principal values of the anisotropic part of the ^{13}C shift tensors of pure BEDT-TTF and α_t-(BEDT-TTF)$_2$I$_3$.

type of carbon	pure BEDT-TTF			α_t-(BEDT-TTF)$_2$I$_3$		
	δ_{xx}	δ_{yy}	δ_{zz}	δ_{xx}	δ_{yy}	δ_{zz}
C_{i1}	27±6	−92±10	65±8	198±8	117±8	−315±9
C_{i2}	19±8	−83±7	63±9	220±16	114±18	−334±16
C_i, average	24±5	−88±6	64±6	209±11	115±10	−324±10
C_{m1}	20±8	−75±5	55±6	125±8	24±6	−149±8
C_{m2}	9±7	−65±8	56±8	107±10	25±11	−132±10
C_{m3}	18±8	−69±8	51±8	119±6	24±5	−143±6
C_{m4}	18±8	−69±8	51±8	142±11	30±12	−172±11
C_m, average	16±7	−70±5	54±6	123±16	26±5	−149±23

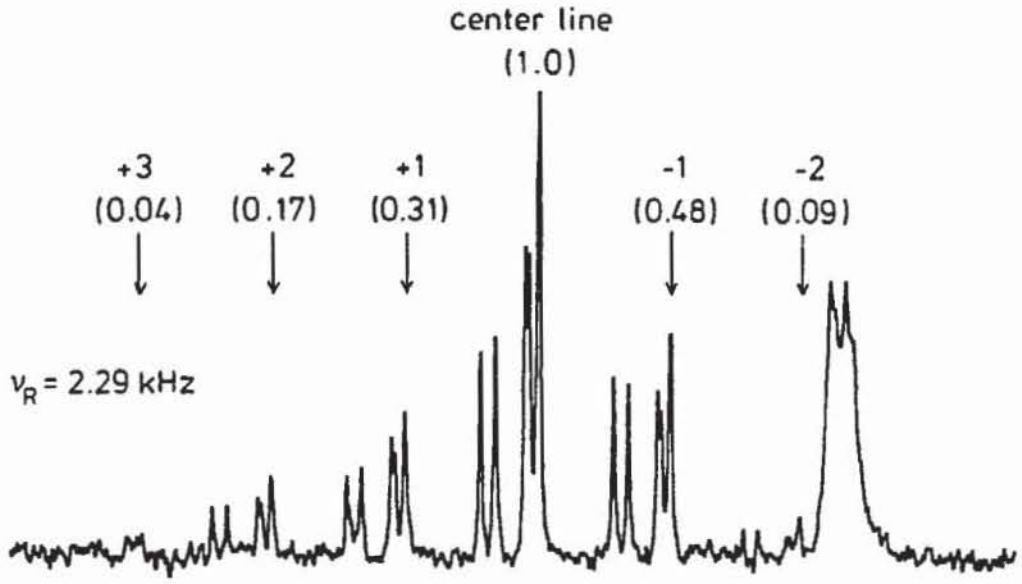

Fig.4. ^{13}C-MASS spectrum of pure BEDT-TTF at a spinning frequency ν_R = 2.29 kHz. The lines marked with arrows are spinning side bands of two of the middle carbons. The numbers in parentheses give the intensities relative to that of the center line.

4.3. Separation of the ^{13}C Shifts in Chemical and Knight Shifts

The ^{13}C shifts δ (shift tensors $\boldsymbol{\delta}$) that can be measured in organic metals such as α_t-(BEDT-TTF)$_2$I$_3$ and (BEDT-TTF)$_2$Cu(NCS)$_2$ are the sum of chemical (σ) and Knight (K) shifts. We must, however, remember that by convention the signs of σ and K are defined differently, therefore

$$\delta = \sigma - K\,. \tag{1}$$

As our eventual goal is information about the π-spin densities at the various carbon and sulphur positions of the BEDT-TTF cations in these organic metals we are primarily interested in the Knight shifts K which originate in the spins of the unpaired electrons. We thus face the task of separating the Knight from the chemical shifts. In their study of the organic metal (fluoranthenyl)$_2$PF$_6$ Wind *et al.* [17] and Stöcklein *et al.* [16] have solved this task by measuring the shifts δ in the *absence* and, in a second run, in the *presence* of a strong microwave field. The first measurement gives $\sigma - K$, the

Table 2. Principal values of the anisotropic part of the average ^{13}C shift tensors of (BEDT-TTF)$_2$Cu(NCS)$_2$.

	$\langle\delta_{xx}\rangle_{av}$	$\langle\delta_{yy}\rangle_{av}$	$\langle\delta_{zz}\rangle_{av}$
C_i, average	142±28	40±18	−182±39
C_m, average	122±8	44±6	−166±10

second one just σ as the strong microwave field saturates the EPR, i.e., leads to $\langle S_z \rangle = 0$ and hence $K = 0$. The difference of the two measurements gives K. (Fluoranthenyl)$_2$PF$_6$ is, however, an exceptionally favourable case for this technique since the extremely narrow EPR line in this quasi one-dimensional organic metal makes it fairly easy to essentially completely saturate the EPR. Here we exploit the well established fact that the *chemical* shift is predominantly an intramolecular and thus a transferable property. The results of [16] and [17] may be taken as a confirmation that this property is also retained when a *neutral* and a *charged* molecule are compared. This means that the chemical shift should essentially be equal in pure BEDT-TTF and in the various metallic radical salts of BEDT-TTF. Therefore we write:

$$-K(\text{metal}) = \delta(\text{metal}) - \sigma(\text{pure BEDT-TTF}), \qquad (2)$$

with metal = α_t-(BEDT-TTF)$_2$I$_3$ and (BEDT-TTF)$_2$Cu(NCS)$_2$.

Equation (2) is, of course, only an approximation. We are going to use Eq.(2) only for the shifts (shift tensors) which are averaged, respectively, over the two inner and four middle carbons. The uncertainty introduced by the approximative character of Eq.(2) can certainly be tolerated in view of the uncertainty resulting from the fact that we cannot assign individual ^{13}C-resonances to individual carbon sites.

The application of Eq.(2) to *isotropic* shifts is straightforward and the results for the C_i and C_m carbons of α_t-(BEDT-TTF)$_2$I$_3$ and (BEDT-TTF)$_2$Cu(NCS)$_2$ are given in Table 3. The error limits in this table have been chosen such that the *largest* and the *smallest* Knight shift in the respective groups of averaged shifts are still covered.

When trying to apply Eq.(2) to the full $\boldsymbol{\delta}$, $\mathbf{K}$ and $\boldsymbol{\sigma}$ tensors we face the problem that the MASS experiment does not provide any information about the orientation of the principal axes system of $\boldsymbol{\delta}$ in the case of the organic metals, and of that of $\boldsymbol{\sigma}$ in the case of pure BEDT-TTF.

Of course one could envisage *measuring* the full ^{13}C shift tensors. This would require taking spectra from crystals for at least 100 different known crystal orientations. The large number of required spectra results from the fact that the spectra would consist in general of as many as 6 (α_t-(BEDT-TTF)$_2$I$_3$), 12 (pure BEDT-TTF) and 24 ((BEDT-TTF)$_2$Cu(NCS)$_2$) resonances from the inner and middle carbons and that therefore only small increments of the rotation angle of the crystals would be tolerable to follow the angular variation of each resonance. We were not able to grow single crystals of either of these materials which were large enough to carry out such a formidable undertaking.

We must thus resort to intuitive, theoretical and symmetry arguments to learn about the orientation of the principal axes systems of $\boldsymbol{\delta}$ and $\boldsymbol{\sigma}$, and about the correspondence between the principal axes and the principal

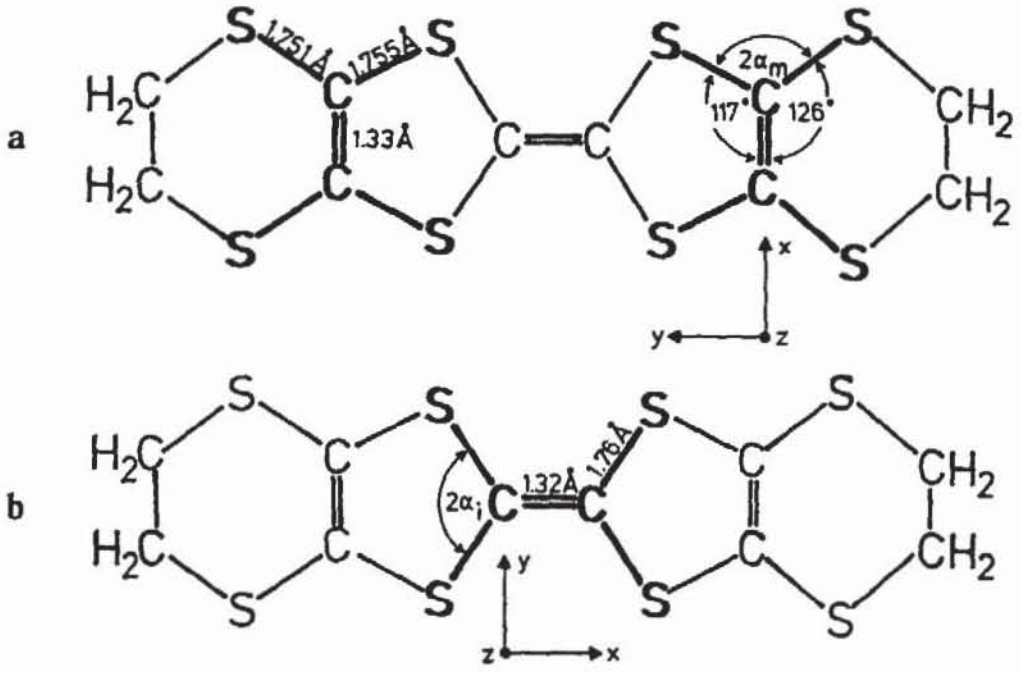

Fig.5. The C_2S_4 fragments (drawn in bold) of the middle (a) and inner carbons (b) of the BEDT-TTF molecule. $2\alpha_i = 113.3°$ and $2\alpha_m = 116°$ [20].

values $\delta_{\alpha\alpha}$ and $\sigma_{\alpha\alpha}$, $\alpha = x,y,z$. We first draw attention to the fact that the local environment of both the inner and middle carbons of BEDT-TTF can be considered to consist of a planar C_2S_4 fragment having approximate D_{2h} symmetry. This is illustrated in Fig.5. The approximation is better for the inner C_2S_4 fragment of which all sulphur atoms are of the S_i type, than for the middle C_2S_4 fragments which contain two S_i and two S_o sulphur atoms.

Within the C_2S_4 fragments with D_{2h} symmetry the carbons are situated on two mutually orthogonal mirror planes. This implies that the principal axes systems of both the $\boldsymbol{\sigma}$ and **K** tensors must coincide, and one principal axis must be perpendicular to the C_2S_4 group, another along the C=C double bond (which is a C_2-axis of the C_2S_4 fragment) and the third perpendicular to the other two.

Knowledge of the orientations of the principal axes systems of $\boldsymbol{\sigma}$ and **K** is, however, still not sufficient for applying Eq.(2) to the full tensors $\boldsymbol{\delta}$, $\boldsymbol{\sigma}$ and **K**. We must know in addition which of the measured principal components of $\boldsymbol{\delta}$ and $\boldsymbol{\sigma}$ (in the case of pure BEDT-TTF) goes with which principal axis.

We first consider pure BEDT-TTF for which $\boldsymbol{\delta} = \boldsymbol{\sigma}$. To assign the measured principal components $\sigma_{\alpha\alpha}$ (see Table 1) to the principal axes we compare the C_2S_4 fragments with the C_2H_4 molecule which has exact D_{2h} symmetry. Note that the carbons in both the C_2S_4 fragments and the C_2H_4 molecule are sp_2 hybridized. It is reasonable to assume that the relation between the *least, intermediate* and *most* shielded directions to the molecular symmetry axes

Table 3. Isotropic Knight shifts of α_t-$(BEDT\text{-}TTF)_2I_3$ and $(BEDT\text{-}TTF)_2Cu(NCS)_2$ relative to pure BEDT-TTF. The Knight shifts of the outer carbons were determined from MASS spectra of unenriched samples using $^1H-^{13}C$ crosspolarization and ^1H decoupling.

	isotropic Knight shifts (ppm)	
	α_t-$(BEDT\text{-}TTF)_2I_3$	$(BEDT\text{-}TTF)_2Cu(NCS)_2$
inner carbons	126, 92 } 109±17	111, 83, 78, 67 } 85±26
middle carbons	63, 52, 44, 34 } 48±15	75, 66[a], 61[b] } 66±11
outer carbons	6, −4.5, −4.5, −4.5 } −2±8	15, 12, 11[a], 9[a], 7, 6 } 10±5

[a] Double intensity.
[b] Triple intensity.

(which are also the principal carbon shielding directions) is the same in the C_2S_4 fragments as in the C_2H_4 molecule. The full ^{13}C chemical shift tensor of C_2H_4 has been calculated by Bouman and Hansen by the quantum chemical RPAC-LORG method [23]. The calculated principal values, +29 ppm, −149 ppm, +120 ppm, agree fairly well with those measured by Zilm *et al.* [24], −3 ppm, −103 ppm, +106 ppm. We may therefore trust that the orientations of least, intermediate and most shielded directions which result from the RPAC-LORG calculation and which are shown in Fig.6a, are correct.

From Table 1 and the comparison with C_2H_4 we conclude that the average chemical shift tensors $\langle\boldsymbol{\sigma}^{(c)}\rangle_{av}$ of the inner (c = i) and middle (c = m) carbons in the BEDT-TTF molecule are oriented as shown in Fig.6b. We point out that the three principal components of $\boldsymbol{\sigma}(C_2H_4)$, $\langle\boldsymbol{\sigma}^{(i)}\rangle_{av}$ and $\langle\boldsymbol{\sigma}^{(m)}\rangle_{av}$ are sufficiently distinct to render the foregoing arguments and conclusions fully trustworthy.

We now turn to the Knight shift tensors $\langle\mathbf{K}^{(c)}\rangle_{av}$ in the metallic BEDT-TTF radical salts. As noted above the principal axes system of $\mathbf{K}$ must coincide for an idealized C_2S_4 fragment with that of $\boldsymbol{\sigma}$. In the following section we shall see that the main contribution to $\mathbf{K}$ of an C_i or C_m carbon in one of the BEDT-TTF radical salts stems from the π-spin density on that very carbon. This implies that the $\mathbf{K}$ tensor of the C_i and C_m carbons should be nearly axially symmetric with the axial symmetry axis perpendicular to the plane of the BEDT-TTF molecule.

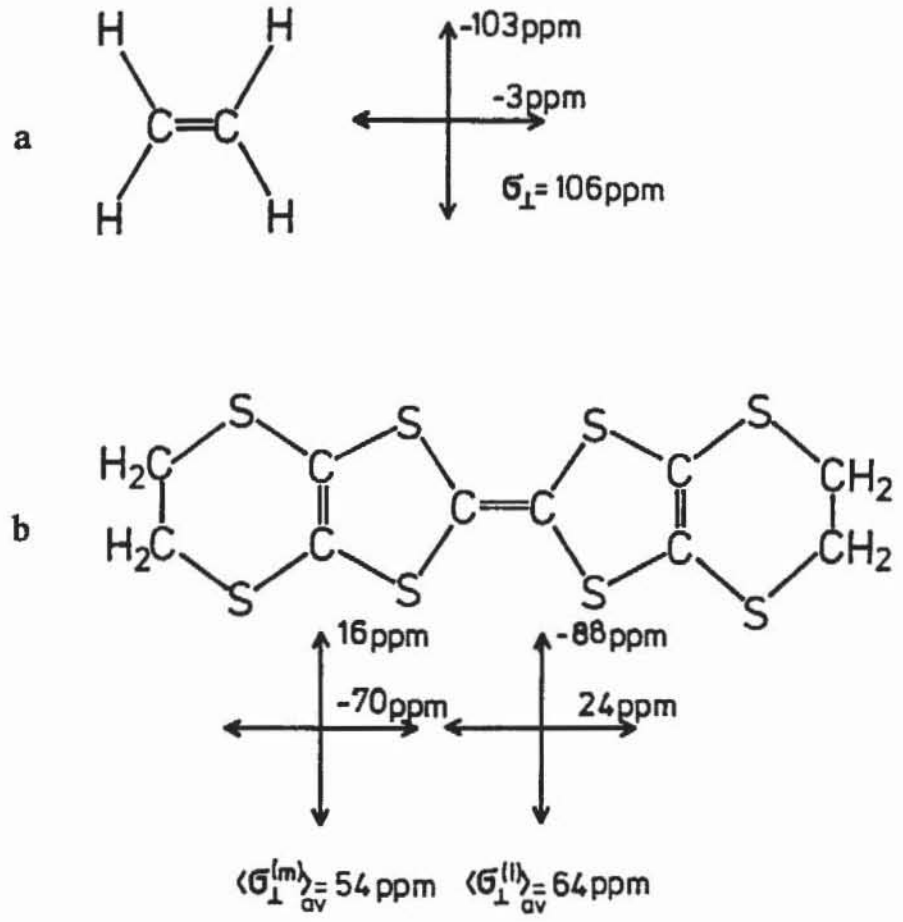

Fig.6. a The C_2H_4 molecule with the principal axes and principal values of the chemical shift tensor σ. b The principal axes and principal values of the chemical shift tensor σ of the middle (left) and inner (right) carbons in pure BEDT-TTF.

Let us now have a closer look at the principal values of $\langle\delta^{(i)}\rangle_{av}$ of α_t-(BEDT-TTF)$_2$I$_3$ and of $\langle\delta^{(i)}\rangle_{av} = \langle\sigma^{(i)}\rangle_{av}$ of pure BEDT-TTF in Table 1. With Eq.(2) in mind their comparison makes immediately clear that, first, $\langle\delta^{(i)}\rangle_{av}$ of α_t-(BEDT-TTF)$_2$I$_3$ is dominated by $\mathbf{K}^{(i)}$ and, second, that the principal direction corresponding to $\langle\delta_{zz}^{(i)}\rangle_{av} = -324$ ppm must be the nearly-axial symmetry axis of $\mathbf{K}^{(i)}$. That means this principal direction must be perpendicular to the molecular plane. This leaves us with only choices (a) and (b) for the other two principal directions. They are illustrated in Fig.7 together with the Knight shift tensors $\mathbf{K}^{(i)}$ which are obtained when for either choice the chemical shift tensor shown in Fig.6b is inserted in Eq.(2).

Clearly only choice (a) is consistent with the requirement that $\mathbf{K}^{(i)}$ should be nearly axially symmetric. Choice (a) therefore is the correct one. This completes the determination of the full Knight shift tensor $\langle\mathbf{K}^{(i)}\rangle_{av}$ of the inner carbons of α_t-(BEDT-TTF)$_2$I$_3$. In an analogous way we have also determined the full Knight shift tensors $\langle\mathbf{K}^{(m)}\rangle_{av}$ of α_t-(BEDT-TTF)$_2$I$_3$ and $\langle\mathbf{K}^{(i)}\rangle_{av}$ and $\langle\mathbf{K}^{(m)}\rangle_{av}$ of (BEDT-TTF)$_2$Cu(NCS)$_2$. They are summarized in Table 4. The errors $\Delta K_{\alpha\alpha}{}^{(c)}$ given in this table were calculated by $\Delta K_{\alpha\alpha}^{(c)} = \sqrt{(\Delta\sigma_{\alpha\alpha}^{(c)})^2+(\Delta\delta_{\alpha\alpha}^{(c)})^2}$, c = i,m.

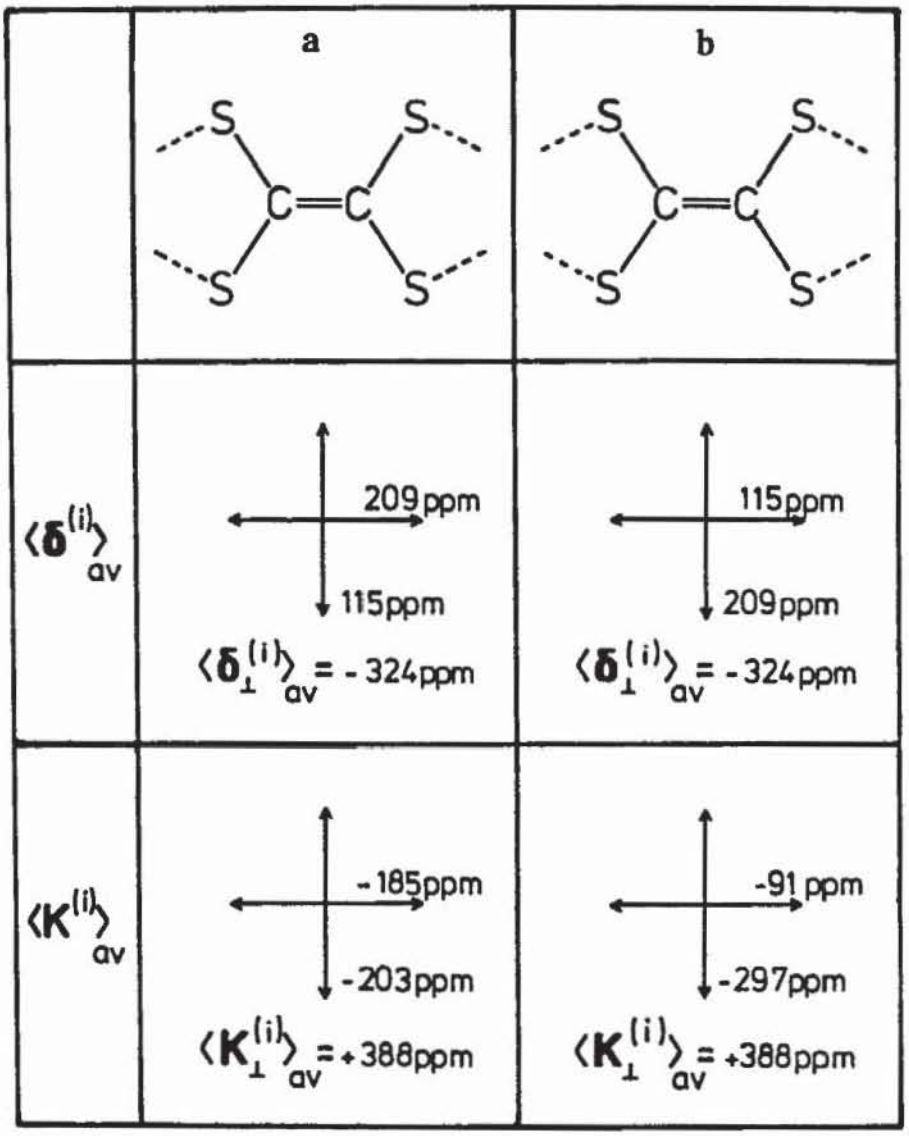

Fig.7. The two possible choices (a) and (b) for the shift tensor $\delta^{(i)}$ and the Knight shift tensor $K^{(i)}$ of the inner carbons of α_t-(BEDT-TTF)$_2$I$_3$. Choice (a) is the correct one as it implies a nearly axially symmetric Knight shift tensor.

4.4. Determination of the π-Spin Densities

Physically the Knight shift results from the coupling of a nuclear spin I with an electronic spin S:

$$\mathscr{H}_{KS}^{op} = \mathbf{I} \cdot \mathbf{a} \cdot \mathbf{S}, \tag{3}$$

where a is the hyperfine coupling tensor. $\mathscr{H}_{KS}^{op}$ in Eq.(3) is an operator with respect to both I and S. Phenomenologically the Knight shift tensor K of a carbon atom c is introduced by:

Table 4. Principal values of the ^{13}C Knight shift tensors of α_t-(BEDT-TTF)$_2$I$_3$ and (BEDT-TTF)$_2$Cu(NCS)$_2$.

		α_t-(BEDT-TTF)$_2$I$_3$	(BEDT-TTF)$_2$Cu(NCS)$_2$
inner carbons	$\langle K_{xx}\rangle_{av}$	(−185±12) ppm	(−118±28) ppm
	$\langle K_{yy}\rangle_{av}$	(−203±12) ppm	(−128±19) ppm
	$\langle K_{zz}\rangle_{av}$	(388±12) ppm	(246±39) ppm
middle carbons	$\langle K_{xx}\rangle_{av}$	(−107±17) ppm	(−106±11) ppm
	$\langle K_{yy}\rangle_{av}$	(−96±7) ppm	(−114±8) ppm
	$\langle K_{zz}\rangle_{av}$	(203±24) ppm	(220±12) ppm

$$\mathcal{H}_{KS} = \hbar\gamma_c \mathbf{I}\cdot\mathbf{K}\cdot\mathbf{B}_0\,, \tag{4}$$

where γ_c is the gyromagnetic ratio of a ^{13}C nucleus and $\mathbf{B}_0$ the applied magnetic field. $\mathcal{H}_{KS}$ is an operator only with respect to the carbon spin operator I. It is related to $\mathcal{H}_{KS}^{op}$ by:

$$\mathcal{H}_{KS} = \langle\mathcal{H}_{KS}^{op}\rangle = \langle\mathbf{I}\cdot\mathbf{a}\cdot\mathbf{S}\rangle = \gamma_c\hbar\mathbf{I}\cdot(\mathbf{a}/\gamma_c\hbar)\cdot\langle\mathbf{S}\rangle\,, \tag{5}$$

where $\langle\ldots\rangle$ means electronic spin expectation value. As the electronic spin or Pauli magnetization per electron spin is

$$\langle\mathbf{M}^{(s)}\rangle = |\gamma_{el}|\hbar\langle\mathbf{S}\rangle = \chi^{(s)}\cdot\mathbf{B}_0\,, \tag{6}$$

we get

$$\langle\mathbf{S}\rangle = (\chi^{(s)}/|\gamma_{el}|\hbar)\cdot\mathbf{B}\,, \tag{7}$$

where $\chi^{(s)}$ is the Pauli susceptibility tensor *per spin*. Combining Eqs.(4), (5) and (7) gives:

$$\mathbf{K} = \mathbf{a}\cdot\chi^{(s)}/\gamma_c|\gamma_{el}|\hbar. \tag{8}$$

The Pauli susceptibility was measured for α_t-(BEDT-TTF)$_2$I$_3$ by Klotz *et al* [12], $\chi^{(s)} = (3.7\pm0.25)\cdot10^{-28}$ emu/molecule, and for (BEDT-TTF)$_2$Cu(NCS)$_2$ by Urayama *et al.* [13], $\chi^{(s)} = (3.8\pm0.25)\cdot10^{-28}$ emu/molecule. Klotz *et al.* [12] also made an effort to measure the anisotropy of $\chi^{(s)}$ and found that it is small in comparison to the isotropic part $\chi^{(s)}$. Therefore in what follows we shall assume that $\chi^{(s)}$ is isotropic.

As regards the hyperfine coupling tensor **a** we first note that we are discussing the traceless part of **K** and hence also the traceless part of **a** which is

the dipolar part $\mathbf{a}_{dip}$ of the hyperfine coupling tensor. We write $\mathbf{a}_{dip}^{(c)}$ of a specific carbon c in the form:

$$\mathbf{a}_{dip}^{(c)} = \mathbf{a}_{dip}^{(c)}(\text{local}) + \sum_{n} \mathbf{a}_{n}^{(c)}, \tag{9}$$

where $\mathbf{a}_{dip}^{(c)}$(local) results from the unpaired π-spin density $\varrho_{\pi c}$ centered on carbon atom c while the $\mathbf{a}_{n}^{(c)}$ result from the π-spin densities $\varrho_{\pi n}$ centered on the other atoms n of the molecule and, in principle, on the atoms of the other molecules in the crystal as well.

$$\mathbf{a}_{dip}^{(c)}(\text{local}) = \mathbf{a}_{2p_z} \cdot \varrho_{\pi c}, \tag{10}$$

where $\mathbf{a}_{2p_z}$ is the dipolar hyperfine coupling tensor of the carbon atom c if the unpaired electron was localized entirely in a $2p_z$ orbital centered on carbon c. For the C_2S_4 fragments we have in mind the z-direction is perpendicular to the fragment's plane. $\mathbf{a}_{2p_z}$ is necessarily axially symmetric, the axial symmetry axis being parallel to z. In the reference frame (x,y,z) shown in Fig.5 for the inner and middle C_2S_4 fragments it will assume the form:

$$\mathbf{a}_{2p_z} = a_1 \begin{pmatrix} -1/2 & 0 & 0 \\ 0 & -1/2 & 0 \\ 0 & 0 & 1 \end{pmatrix} \text{ with } a_1 = \frac{4}{5}\hbar^2 \gamma_c |\gamma_{el}| \cdot \left\langle \frac{1}{r_e^3} \right\rangle, \tag{11}$$

where $\langle 1/r_e^3 \rangle$ is the expection value of $1/r_e^3$ taken over the $2p_z$ orbital [25]. For a *carbon* $2p_z$ orbital $\langle 1/r_e^3 \rangle = 11.49$ Å^{-3} or $1/\sqrt[3]{\langle 1/r_e^3 \rangle} = 0.443$ Å [26].

For estimating the partial coupling tensors $\mathbf{a}_{n}^{(c)}$ in Eq.(9) we assume that the π-spin density $\varrho_{\pi n}$ centered on an atom n is concentrated at the site of the nucleus n (point dipole approximation) [14]. $\mathbf{a}_{n}^{(c)}$ is then nothing else than the dipolar coupling tensor between two point dipoles $\gamma_c \hbar \mathbf{I}$ and $|\gamma_{el}| \hbar \mathbf{S} \varrho_{\pi n}$ separated by the internuclear vector $\mathbf{r}_{cn}$. The p,q-component of $\mathbf{a}_{n}^{(c)}$ is given by:

$$\mathbf{a}_{n}^{(c)}(p,q) = -\frac{\gamma_c |\gamma_{el}| \hbar^2 \varrho_{\pi n}}{r_{cn}^3} \left(\delta_{pq} - \frac{3 x_p x_q}{r_{cn}^2} \right), \tag{12}$$

where x_p and x_q are, respectively the p and q components of $\mathbf{r}_{cn}$, and $r_{cn} = |\mathbf{r}_{cn}|$. Because $\mathbf{a}_{n}^{(c)}$ decreases with the inverse cube of r_{cn} we restrict the summation in Eq.(9) to atoms which are directly bonded to the carbons of interest, i.e., C_i and C_m. The geometric information needed to evaluate the $\mathbf{a}_{n}^{(i)}$ and $\mathbf{a}_{n}^{(m)}$ is provided in Fig.5.

We are now in a position to express the principal components of $K_{xx}^{(i)}$, $K_{yy}^{(i)}$ and $K_{zz}^{(i)} \equiv K_{\perp}^{(i)}$ in terms of the π-spin densities $\varrho_{\pi i}$ and $\varrho_{\pi s_i}$ centered on the inner carbon and sulphur atoms of the BEDT-TTF molecule with all coefficients being *known* quantities:

$$K_{xx}^{(i)} = \chi^{(s)}\left\{\left(-\frac{2}{5}\left\langle\frac{1}{r_e^3}\right\rangle + \frac{2}{r_{cc}^3}\right)\varrho_{\pi i} + \frac{2(3\cos^2\alpha - 1)}{r_{cs}^3}\varrho_{\pi s_i}\right\}, \tag{13a}$$

$$K_{yy}^{(i)} = \chi^{(s)}\left\{\left(-\frac{2}{5}\left\langle\frac{1}{r_e^3}\right\rangle - \frac{1}{r_{cc}^3}\right)\varrho_{\pi i} + \frac{2(3\cos^2\alpha - 1)}{r_{cs}^3}\varrho_{\pi s_i}\right\}, \tag{13b}$$

$$K_{zz}^{(i)} = \chi^{(s)}\left\{\left(+\frac{4}{5}\left\langle\frac{1}{r_e^3}\right\rangle - \frac{1}{r_{cc}^3}\right)\varrho_{\pi i} + \frac{2}{r_{cs}^3}\varrho_{\pi s_i}\right\}. \tag{13c}$$

The first term in each of these expression comes from the local spin density centered on the carbon atom i whose Knight shift tensor we are considering. The second comes from the carbon atom, and the last from the *two* sulphur atoms bonded to carbon i. As we cannot distinguish the two inner carbons by their chemical and Knight shifts it is just consequent to assign the *same* π-spin densities $\varrho_{\pi i}$ to both inner carbons and the *same* $\varrho_{\pi s_i}$ to all inner sulphurs, as we have done in Eqs.(13a)-(13c).

Since $\langle 1/r_e^3\rangle$ is very much larger than $1/r_{cc}^3$ and $1/r_{cs}^3$ the Knight shift tensor $\mathbf{K}^{(i)}$ is dominated by the *local* term which *alone* would give an axially symmetric tensor. This is why the preceding section we set up the requirement that $\mathbf{K}^{(i)}$ (and also $\mathbf{K}^{(m)}$ should be nearly axially symmetric.

Turning now to the Knight shift tensor $\mathbf{K}^{(m)}$ of the middle carbons of the BEDT-TTF molecule we can set up equations analogous to Eqs.(13a)-(13c) simply by replacing $\varrho_{\pi i}$ by $\varrho_{\pi m}$ and $2 \cdot \varrho_{\pi s_i}$ by $(\varrho_{\pi s_i} + \varrho_{\pi o})$. There is, however, a problem: as the two sulphurs bonded to a middle carbon are different even in our simplified description where all inner and outer sulphurs, respectively, are considered as equivalent, the x,y,z frame in Fig.5 will not be exactly the principal axes system of $\mathbf{K}^{(m)}$ which means there will also be a nonzero $K_{xy}^{(m)}$ tensor element. As before $K_{xz}^{(m)} = K_{yz}^{(m)} = 0$ because also the middle C_2S_4 group may be considered to be planar. Here we shall neglect the $K_{xy}^{(m)}$ element and shall show later on that this is justified.

By inserting the *measured* principal components of $\langle \mathbf{K}^{(i)}\rangle_{av}$ and $\langle \mathbf{K}^{(m)}\rangle_{av}$ from α_t-(BEDT-TTF)$_2$I$_3$ in Eqs.(13a)-(13c) and the analogous ones for $\langle \mathbf{K}^{(m)}\rangle_{av}$ and inserting numbers for the coefficients we get the following set of equations for the π-spin densities $\varrho_{\pi i}$, $\varrho_{\pi m}$, $\varrho_{\pi s_i}$ and $\varrho_{\pi s_o}$:

$$\langle K_{xx}^{(i)}\rangle_{av} = -(185 \pm 12) = -1371\varrho_{\pi i} - 29\varrho_{\pi s_i}, \tag{14a}$$

$$\langle K_{yy}^{(i)}\rangle_{av} = -(203 \pm 12) = -1854\varrho_{\pi i} + 148\varrho_{\pi s_i}, \tag{14b}$$

$$\langle K_{zz}^{(i)}\rangle_{av} = +(388\pm12) = +3225\varrho_{\pi i} - 136\varrho_{\pi s_i}, \tag{14c}$$

$$\langle K_{xx}^{(m)}\rangle_{av} = -(107\pm17) = -1379\varrho_{\pi m} + 19(\varrho_{\pi s_i}+\varrho_{\pi s_o}), \tag{15a}$$

$$\langle K_{yy}^{(m)}\rangle_{av} = -(96\pm7) = -1850\varrho_{\pi m} + 121(\varrho_{\pi s_i}+\varrho_{\pi s_o}), \tag{15b}$$

$$\langle K_{zz}^{(m)}\rangle_{av} = -(203\pm24) = +3229\varrho_{\pi m} - 140(\varrho_{\pi s_i}+\varrho_{\pi s_o}). \tag{15c}$$

All shifts and coefficients are expressed in ppm. In addition to these equations we have the normalization condition:

$$\sum_k \varrho_{\pi k} = 2\varrho_{\pi i} + 4\varrho_{\pi s_i} + 4\varrho_{\pi m} + 4\varrho_{\pi s_o} = 1. \tag{16}$$

In Eq.(16) we assumed that the π-spin density on the outer carbons C_o of the BEDT-TTF molecule is negligibly small. This assumption is justified by the observation that the anisotropy of the Knight shift tensor of the C_o carbons is below detectability in the MASS experiment, but also by just noting that these carbons are sp_3 hybridized and do not contribute to the delocalized π-electron system. Eqs.(14a) through (16) represent an overdetermined set seven equations for the four unknowns $\varrho_{\pi i}$, $\varrho_{\pi m}$, $\varrho_{\pi s_i}$ and $\varrho_{\pi s_o}$. We solve it in the following way: Since Eq.(16) is without experimental errors we use it to eliminate one of the unknowns. We then minimize the expression:

$$(-1371\varrho_{\pi i} - 29\varrho_{\pi s_i} + 185)^2 + \ldots(\text{total of six terms})\ldots, \tag{17}$$

which can be done analytically. The result for α_t-$(BEDT\text{-}TTF)_2I_3$ is:

$$\varrho_{\pi i} = 0.131, \qquad \varrho_{\pi s_i} = 0.252,$$
$$\varrho_{\pi m} = 0.067, \qquad \varrho_{\pi s_o} = -0.135,$$
$$\varrho_{\pi o} = 0.0.$$

It is now very important to note that these values for the π-spin densities *solve all of* Eqs.(14a)-(15c) *within the specified error limits* of the measured Knight shifts $K_{\alpha\alpha}^{(c)}$, c = i,m; $\alpha = x,y,z$. They also fulfill, of course, the normalization condition. Conservative estimates for the error limits are:

$$\Delta\varrho_{\pi i} = \pm0.006, \quad \Delta\varrho_{\pi m} = \pm0.018 \quad \text{and} \quad \Delta(\varrho_{\pi s_i}+\varrho_{\pi s_o}) = \pm0.019.$$

We give an error limit for $(\varrho_{\pi s_i}+\varrho_{\pi s_o})$ rather than for the individual π-spin densities on the sulphur atoms because it is this sum which can be determined rather reliably while the individual errors are substantially larger.

Further up we mentioned that the axes x,y,z of the reference frame shown in Fig.5 are *not* the principal axes of $\langle \mathbf{K}^{(m)} \rangle_{av}$ and that the element $\langle K_{xy}^{(m)} \rangle_{av}$ is nonzero. By inserting $\varrho_{\pi m}$, $\varrho_{\pi s_i}$ and $\varrho_{\pi s_o}$ and the coordinates x_x and x_y of the atoms bonded to $C^{(m)}$ into Eqs.(12) and (9) we may now estimate the size of $\langle K_{xy}^{(m)} \rangle_{av}$. The result is $\langle K_{xy}^{(m)} \rangle_{av} / \langle K_{xx}^{(m)} \rangle_{av} \approx 1/7$ and $\langle K_{xy}^{(m)} \rangle_{av} / \langle K_{yy}^{(m)} \rangle_{av} \approx 1/9$ which means it was justified neglecting $\langle K_{xy}^{(m)} \rangle_{av}$.

In the same way as described here for α_t-(BEDT-TTF)$_2$I$_3$ we determined the π-spin densities at the carbon and sulphur positions of (BEDT-TTF)$_2$Cu(NCS)$_2$. The results for (BEDT-TTF)$_2$Cu(NCS)$_2$ are:

$$\begin{aligned} \varrho_{\pi i} &= 0.082\,, & \varrho_{\pi s_i} &= 0.155\,, \\ \varrho_{\pi m} &= 0.074\,, & \varrho_{\pi s_o} &= -0.02\,, \\ \varrho_{\pi o} &= 0.0\,, \end{aligned}$$

with the following error limits:

$$\Delta\varrho_{\pi i} = \pm 0.027\,,\ \Delta\varrho_{\pi m} = \pm 0.024 \text{ and } \Delta(\varrho_{\pi s_i} + \varrho_{\pi s_o}) = \pm 0.028\,.$$

The error limits are *larger* than for α_t-(BEDT-TTF)$_2$I$_3$. This is due to the fact that the Knight shift tensors among the inner and middle carbons differ substantially more in (BEDT-TTF)$_2$Cu(NCS)$_2$ than they do in α_t-(BEDT-TTF)$_2$I$_3$.

4.5. π-Spin Densities and Isotropic Knight Shifts

Isotropic Knight shifts arise from the Fermi contact interaction between the electronic spin **S** and nuclear spins **I**. They also depend linearly on the distribution of the π-spin density. Following Carrington and McLachlan [25,chapt.6] we write:

$$\langle K^{(i)} \rangle_{av} = \chi^{(s)} \{ (k_c + k_{cc}) \varrho_{\pi i} + 2 k_{cs} \varrho_{\pi s_i} \}\,, \tag{18a}$$

$$\langle K^{(m)} \rangle_{av} = \chi^{(s)} \{ (k_c + k_{cc}) \varrho_{\pi m} + k_{cs} (\varrho_{\pi s_i} + \varrho_{\pi s_o}) \}\,, \tag{18b}$$

$$\langle K^{(o)} \rangle_{av} = \chi^{(s)} \cdot k'_{cs} \varrho_{\pi s_o}\,. \tag{18.c}$$

These equations express the idea that the isotropic Knight shift of one of the carbons C_i, C_m or C_o depends linearly on the π-spin densities centered on those atoms which are directly bonded to the carbon under consideration while the contribution from π-spin densities centered on atoms further away may be neglected. For simplicity we used the same coefficients k_c, k_{cc} and

k_{cs} for the inner and middle carbons while this would be too gross an approximation for the outer carbon C_o which is sp_3 hybridized. In Eq.(18c) we therefore used a different coefficient k'_{cs}. Unlike to the case of the dipole-dipole interaction between **S** and **I**, we cannot calculate from geometric considerations the coefficients k_c, k_{cc}, k_{cs} and k'_{cs}. Therefore we cannot use Eqs.(18a)-(18c) for determining the π-spin densities $\varrho_{\pi i}$, $\varrho_{\pi m}$, $\varrho_{\pi s_i}$ and $\varrho_{\pi s_o}$ from the measured isotropic Knight shifts. However, by inserting $\varrho_{\pi i}$, $\varrho_{\pi m}$, $\varrho_{\pi s_i}$ and $\varrho_{\pi s_o}$ obtained in Section 4.4 in Eqs.(18a) and (18b) and inserting the measured Knight shifts from Table 3 in the left hand side we are now in a position to determine the coefficients (k_c+k_{cc}) and k_{cs}. Inserting numbers in these equations and solving for $\chi^{(s)}(k_c+k_{cc})$ and $\chi^{(s)}k_{cs}$ gives:

$$\chi^{(s)} \cdot (k_c+k_{cc}) = 620\,\text{ppm} \quad \text{and}$$
$$\chi^{(s)} \cdot k_{cs} = 55\,\text{ppm}.$$

However, within the error limits specified in Table 3 for $\langle K^{(i)}\rangle_{av}$ and $\langle K^{(m)}\rangle_{av}$ Eqs.(18a) and (18b) may also be satisfied by setting $k_{cs} = 0$. In any event the ratio $k_{cs}/(k_c+k_{cc})$ is a *small* number. This implies that a meaningful estimate of the ratio $\varrho_{\pi m}/\varrho_{\pi i}$ can be obtained from the isotropic Knight shifts $\langle K^{(i)}\rangle_{av}$ and $\langle K^{(m)}\rangle_{av}$ *alone*. This result may be taken as a justification of the tacit assumption $k_{cs} = 0$ made by Vainrub *et al.* [14] in their effort to estimate the π-spin densities in β-$(BEDT\text{-}TTF)_2I_3$. We point out that the analogous assumption $k_{cc}/k_c \ll 1$ would be grossly *incorrect*, cf. Carrington-McLachlan [25,p.94] and Karplus and Fraenkel [27].

Inserting $\varrho_{\pi s_o}$ from Section 4.4 together with the measured value for $\langle K^{(o)}\rangle_{av}$ into Eq.(18c) leads to the conclusion that $\chi^{(s)} \cdot k'_{cs}$ as well is very small. As the error limits also permit $\langle K^{(o)}\rangle_{av}$ to be positive it is well possible that k'_{cs} is small and *negative*. Theory [27] and comparison with other systems [25,27] suggest that k'_{cs} and also k_{cs} should be *negative*.

5. Discussion

We have shown in Section 4 that the π-spin densities centered on the carbon as well as those centered on the sulphur atoms of the BEDT-TTF molecule can be determined with reasonable accuracy from the *anisotropic* parts of the Knight shift tensors **K** of the carbon atoms *alone*. Fig.8 is an attempt to represent graphically the π-spin densities obtained in this way for α_t-$(BEDT\text{-}TTF)_2I_3$ and $(BEDT\text{-}TTF)_2Cu(NCS)_2$. For α_t-$(BEDT\text{-}TTF)_2I_3$ the π-spin densities $\varrho_{\pi i}$ and $\varrho_{\pi m}$ of the middle carbons are definitively and the relative uncertainties $\Delta\varrho_{\pi i}/\varrho_{\pi i}$ and $\Delta\varrho_{\pi m}/\varrho_{\pi m}$ are rather small. As regards the π-spin densities of the inner and outer sulphur atoms only the sum $(\varrho_{\pi s_i}+\varrho_{\pi s_o})$ can be determined with comparable accuracy. Nevertheless it is

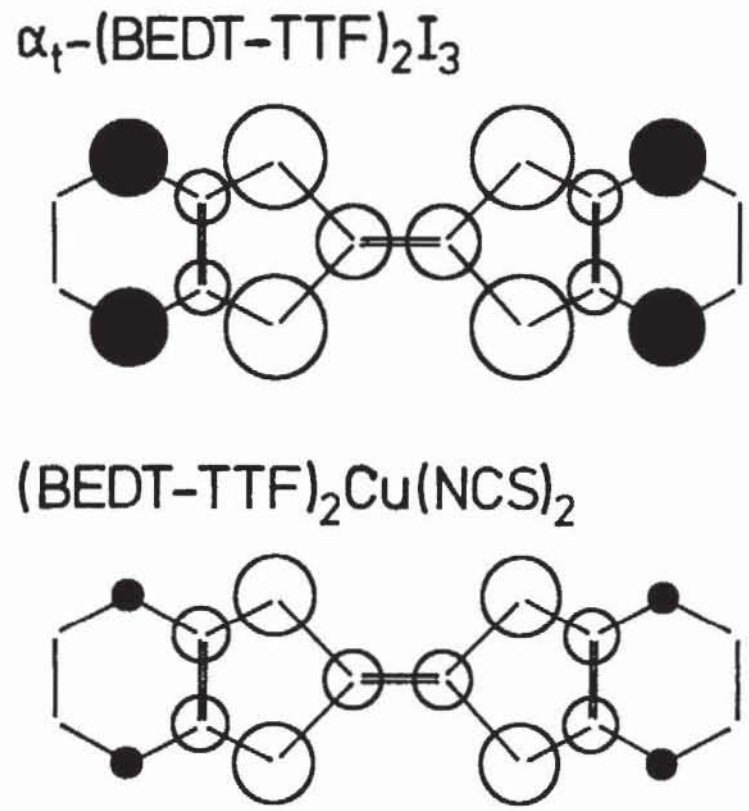

Fig.8. The illustration of π-spin densities of α_t–(BEDT–TTF)$_2$I$_3$ and (BEDT–TTF)$_2$Cu(NCS)$_2$. Positive (negative) π-spin densities are shown by open (full) circles. The *area* of the circles are proportional to the π-spin density centered at the respective atom.

clear that the π-spin density $\varrho_{\pi s_i}$ centered on the *inner* sulphur atoms is positive whereas the π-spin density $\varrho_{\pi s_o}$ centered on the *outer* sulphur atoms is negative. As in α_t-(BEDT-TTF)$_2$I$_3$ and other metallic radical salts based on BEDT-TTF this molecule carries a *positive* charge we are actually discussing the distribution of an unpaired *hole* in a delocalized π-orbital. We note in passing that it is a (BEDT-TTF)$_2$ *dimer* which carries one positive elementary charge, nevertheless we have normalized the π-spin density to unity over one *molecule*. We have taken care of this by referring the Pauli susceptibility as well to one molecule.

If the π-spin density were distributed *evenly* over all inner middle carbons, and all inner and middle sulphur atoms of the BEDT-TTF molecule all these π-spin densities would be 0.10. We thus conclude that the delocalized unpaired spin in α_t-(BEDT-TTF)$_2$I$_3$ is *overrepresented* at the inner carbon and sulphur atoms and *underrepresented* at the middle carbons. The negative π-spin density obtained for the outer sulphur atoms means that the delocalized unpaired π-hole essentially is absent at these outer sulphur atoms and that a magnetic moment opposite to that of the delocalized unpaired π-hole appears at these atoms only through electron-electron correlation effects. As pointed out in the introduction the short intermolecular sulphur-sulphur distances which exist between the inner and outer sulphur atoms are thought to provide the contacts needed to permit a macroscopic charge

transport. By contrast, the π-spin density distribution which we inferred from the ^{13}C Knight shift tensors shows clearly that the mobile hole and therefore the charge transport through the metallic radical salts based on BEDT-TTF is essentially confined to the inner carbon and sulphur atoms. The short interatomic distances involving outer sulphur atoms seem to play a negligible role for the charge transport. Basically the same result is obtained for $(BEDT\text{-}TTF)_2Cu(NCS)_2$. The only noteable difference to $\alpha_t\text{-}(BEDT\text{-}TTF)_2I_3$ is that in this salt the π-spin densities at the middle and inner carbons are about equal while that of the outer sulphurs is almost zero.

Acknowledgements

This work is part of a research program on organic superconductors which is carried out in collaboration with the group of H.J.Keller of the Anorganisch-Chemisches Institut der Universität Heidelberg. We are indebted to Ilsabe Heinen for the synthesis of ^{13}C-enriched BEDT-TTF and the growth of the radical BEDT-TTF salts. We would like to thank Heike Kessel for her help with the data analysis and preparing the figures.

References

[1] Bender, K., Dietz, K., Endres, H., Hellberg, H.W., Hennig, I., Keller, H.J., Schäfer, H.W., Schweitzer, D.: Mol. Cryst. Liq. Cryst. **107**, 45–53 (1984)
[2] Bender, K., Hennig, I., Schweitzer, D., Dietz, K., Endres, H., Keller, H.J.: Mol. Cryst. Liq. Cryst. **108**, 359–371 (1984)
[3] Yagubskii, E.B., Schegolev, I.T., Laukhin, V.N., Kononovich, P.A., Kartsovnic, M.V., Zvaryknia, A.V., Buravov, C.I.: Pis'ma Zh. Eksp. Teor. Fiz. **39**, 12–15 (1984)
[4] Baram, G.O., Buravov, L.I., Degtyarev, L.C., Koszlov, M.E., Laukhin, V.N., Laukhin, E.E., Orischenko, V.G., Pokhodnya, K.I., Scheinkman, M.K., Shibaeva, R.P., Yagubskii, E.B.: Pis'ma Zh. Eksp. Teor. **44**, 293–294 (1986)
[5] Schweitzer, D., Bele, P., Brunner, H., Gogu, E., Haeberlen, U., Hennig, I., Klutz, T., Swietlik, R., Keller, H.J.: Z. Phys. B **67**, 489–495 (1987)
[6] Schweitzer, D., Gogu, E., Hennig, I., Klutz, T., Keller, H.J.: Br. Bunsenges. Phys. Chem. **91**, 890–896 (1987)
[7] Endres, H., Müller, M., Keller, H.J., Bender, K., Gogu, E., Heinen, I., Schweitzer, D.: Z. Naturforschung **40b**, 1664–1671 (1985)
[8] Emge, T.J., Wang, H.H., Geiser, U., Beno, M.A., Webb, K.S., Williams, J.M.: J. Amer. Chem. Soc. **108**, 3849–3850 (1986)
[9] Urayama, H., Yamochi, H., Saito, G., Sato, S., Kawamoto, A., Tanaka, J.: Chem. Lett., 463–466 (1988)
[10] Urayama, H., Yamochi, H., Saito, G., Nozawa, K., Sugano, T., Kinoshita, M., Sato, S., Oshina, K., Kawamoto, A., Tanaka, J.: Chem. Lett., 55–58 (1988)
[11] Gärtner, S., Gogu, E., Heinen, I., Keller, H.J., Klutz, T., Schweitzer, D.: Solid State Comm. **65**, 1531–1534 (1988)
[12] Klotz, S., Schilling, J.S., Gärtner, S., Schweitzer, D.: Solid State Comm. **67**, 981–984 (1988)

[13] Urayama, H., Yamochi, H., Saito, G., Sugano, T., Kinoshita, M., Inabe, T., Mori, T., Maruyama, Y., Inokushi, H.: Chem. Lett., 1057–1060 (1988)
[14] Vainrub, A.M., Kheinmaa, I.A., Yagubskii, E.B.: Pis'ma Zh. Eksp. Teor. Fiz. **44**, 247–249 (1986)
[15] Mehring, M., Spengler, J.: Phys. Rev. Lett. **53**, 2441–2444 (1984)
[16] Stöcklein, W., Seidel, H., Singel, D., Kendrick, D., Yannoni, C.S.: Chem. Phys. Lett. **141**, 277–282 (1987)
[17] Wind, R.A., Lock, H., Mehring, M.: Chem. Phys. Lett. **141**, 283–288 (1987)
[18] Köngeter, D., Hentsch, F., Seidel, H., Mehring, M., von Schütz, J.U., Wolf, H.C., Erk, P., Hünig, S.: Solid State Comm. **65**, 453–456 (1988)
[19] Bernier, P., Audenaert, M., Schweizer, R.J., Stein, P.C., Jérome, D., Bechgaard, K., Moradpour, A.: J. Physique Lett. **46**, L675–L681 (1985)
[20] Kobayashi, H., Kobayashi, A., Sasaki, Y., Saito, G., Inokushi, H.: Bull. Chem. Soc. Jpn. **59**, 301–302 (1986)
[21] Raleigh, D.P., Olejniczak, E.T., Vega, S., Griffin, R.G.: J. Magn. Res. **72**, 238–250 (1987)
[22] Herzfeld, J., Berger, A.: J. Chem. Phys. **73**, 6021–6030 (1980)
[23] Hansen, A.E., Bouman, T.D.: J. Chem. Phys. **82**, 5035–5047 (1985)
[24] Zilm, K.W., Grant, D.M.: J. Amer. Chem. Soc. **103**, 2913–2922 (1981)
[25] Carrington, A., McLachlan, A.D.: Introduction to Magnetic Resonances, New York: Harper & Row 1969.
[26] Symons, M.: Chemical and Biochemical Asprcts of Electron-Spin Resonance Spectroscopy, Wokingham, Berkshire, England: Van Nostrand Reinhold Company 1978.
[27] Karplus, M., Fraenkel, G.K.: J. Chem. Phys. **35**, 1312–1323 (1961)

Author's address: Prof. Dr. U.Haeberlen, Max-Planck-Institut für Medizinische Forschung, Arbeitsgruppe Molekülkristalle, Jahnstraße 29, 6900 Heidelberg, Germany